

***Ab Initio* Molecular Dynamics with Variable Cell Shape: Application to MgSiO₃**Renata M. Wentzcovitch,⁽¹⁾ José Luís Martins,^{(2),(3)} and G. D. Price⁽⁴⁾⁽¹⁾*Cavendish Laboratory, University of Cambridge, Cambridge, CB3 0HE, United Kingdom*⁽²⁾*Departamento de Física, Instituto Superior Técnico, Av. Rovisco Pais 1, 1096 Lisboa codex, Portugal*⁽³⁾*INESC, Rua Alves Redol 9, 1017 Lisboa codex, Portugal*⁽⁴⁾*Research School of Geological and Geophysical Sciences, Birkbeck College, University College London, Gower Street, London, WC1E 6BT, United Kingdom*

(Received 15 January 1993)

We report the development of an *ab initio* constant pressure extended molecular dynamics method with variable cell shape. This is a symmetry conserving method which allows for efficient structural searches and optimizations in spaces with preselected symmetry groups. We have used it to investigate MgSiO₃ a perovskite, the major Earth-forming mineral phase which exists particularly in the lower mantle. We predict its structural behavior up to pressures which exceed the highest values reached in this region.

PACS numbers: 71.20.Ad, 62.50.+p, 64.30.+t

The advent of *ab initio* molecular dynamics [1] in recent years has not only renewed our theoretical approaches to address theoretical materials' problems but has also rejuvenated our views within both subjects: electronic structure and molecular dynamics (MD). In this Letter we report a further development which extends the *ab initio* approach to the constant pressure MD with variable cell shape [2]. We start from an extended Lagrangian formulation which includes also "strains" as dynamical variables [3], and combine it with an efficient and accurate *ab initio* MD [4]. We arrive at a versatile algorithm for the simulation of materials under constant pressure which leaves thermal fluctuations of atomic positions as the only symmetry breaking mechanism. This type of dynamics is of extraordinary importance to high pressure mineral physics and, accordingly, we demonstrate its application to MgSiO₃, the most abundant mineral on our planet. Latest estimates suggest that at least 85% of the Earth's lower mantle consists of pure perovskite Mg_{1-x}Fe_xSiO₃ ($x \leq 0.2$) [5]. This is the largest single region of the planet and accounts for $\approx 55\%$ of its volume; however, the precise behavior of this mineral under this region's extreme conditions is as yet unknown. We apply this algorithm to perform symmetry conserving structural optimizations and predict the zero temperature behavior of this mineral up to pressures which exceed the highest values reached within the Earth's mantle.

Ab initio predictions of relative structural stabilities under pressure are based on tractable total energy schemes [6] making use of the local density approximation (LDA) to density functional theory. Early investigations involved static configurations of ions (at constant volumes) and the search for the optimal configuration was essentially educated guess work. The introduction of *ab initio* MD by Car and Parrinello [1] (CP) has made possible efficient and less constrained structural optimization of internal parameters, but still within this constant volume strategy. Their algorithm also offered the possibility of performing finite temperature MD. Our basic

MD method [4], in common with other recent works [7], differs from the CP scheme by using a more traditional MD time step and fully converged LDA energies, forces, and stresses at every step. In common with CP and all the other *ab initio* MD approaches, we use (a) pseudopotentials in conjunction with a plane-wave basis set, (b) iterative improvement of trial electronic wave functions, and (c) fast Fourier transform convolutions in the operation of the potential on the wave functions. However, when the cell shape is variable, we impose a constant energy cutoff for plane-wave expansions and allow for a variable number of basis functions.

The present technique goes beyond previous implementations and includes the Bravais lattice "deformations" among the dynamical variables. The combination of a new version of variable cell shape dynamics [3], with our efficient first principles MD [4], has resulted in an accurate and versatile algorithm to perform constant pressure simulations and structural optimizations under pressure. In general [2], this type of dynamics proceeds in a space with variable metric where the ionic coordinates are referenced to a "breathing" frame. Specifically, this recent formulation [3] takes advantage of strains and rescales the ionic coordinates (\mathbf{r}_i) by $\mathbf{r}_i(\epsilon, \mathbf{q}_i) = (1 + \epsilon)\mathbf{q}_i$, where ϵ is the (second rank) strain tensor [8]. An extended Lagrangian is then formulated by promoting the strain components and the rescaled ionic coordinates (\mathbf{q}_i) to dynamical variables:

$$L = \sum_{i=1}^N \frac{m_i}{2} \dot{\mathbf{q}}_i g(\epsilon) \dot{\mathbf{q}}_i + \frac{w}{2} \text{Tr}(\dot{\epsilon} \dot{\epsilon}^T) - U(\epsilon, \mathbf{q}_i) - P \Omega(\epsilon). \quad (1)$$

Here $g(\epsilon) = (1 + \epsilon)^T (1 + \epsilon)$ is the metric tensor, $U(\epsilon, \mathbf{q}_i)$ is the Kohn-Sham energy, P is the constant applied external pressure, and $\Omega(\epsilon)$ is the variable cell volume. The first and second terms on the right-hand side are the kinetic energies associated with internal and strain variables (w is a *fictitious* mass usually adjusted to optimize the dynamical coupling with the other variables). The third and fourth terms combined correspond to the

enthalpy which plays the role of a generalized potential energy. Structural optimization at arbitrary pressures can therefore be achieved by minimizing the enthalpy along trajectories generated by the following equations of motion (EM):

$$\ddot{\mathbf{q}}_i = -\frac{1}{m_i}(1+\epsilon)^{-1}\mathbf{f}_i - \mathbf{g}^{-1}\dot{\mathbf{g}}\dot{\mathbf{q}}_i, \quad (2a)$$

$$\dot{\epsilon} = \frac{\Omega}{w}(\Pi - P)(1+\epsilon^T)^{-1}. \quad (2b)$$

In Eq. (2a), \mathbf{f}_i 's are the Hellmann-Feynman forces, and in (2b), Π is the total stress:

$$\Pi = \sum_{i=1}^N \frac{1}{\Omega} m_i \mathbf{v}_i \mathbf{v}_i^T + \Sigma, \quad (3)$$

where $\mathbf{v}_i(\epsilon, \dot{\mathbf{q}}_i) = (1+\epsilon)\dot{\mathbf{q}}_i$ and Σ is the quantum mechanical stress tensor [9]. In the absence of thermal fluctuations ($\mathbf{v}_i = 0$ for all i 's), the dynamical part of the stress tensor [first term on the right-hand side of Eq. (3)] is free of random components, which implies symmetry conserving trajectories [10]. This property is advantageous because it guarantees the invariance of the irreducible Brillouin zone (IBZ) wedge and of the \mathbf{k} point set, from which symmetrized quantities can be obtained similarly at every step. Besides, it is not restrictive, since the initial configuration may not have symmetry, and more symmetrical configurations are particular cases not excluded from the trajectories. Although we have used this dynamics only as an optimization strategy, finite temperature simulations can also be generated.

Because of the relatively large degree of structural freedom, orthorhombic MgSiO_3 perovskite ($Pbnm$) is an ideal test material for the present method. This phase is stable above 23 GPa [11], which is the typical pressure at the upper/lower mantle boundary. At lower pressures it is metastable, the stabler phases being pyroxenes. The orthorhombic phase [Fig. 1(b)] is obtained from the hypothetical cubic perovskite phase ($Pm\bar{3}m$) [Fig. 1(a)] by superposing rotations of nearly rigid oxygen octahedra to

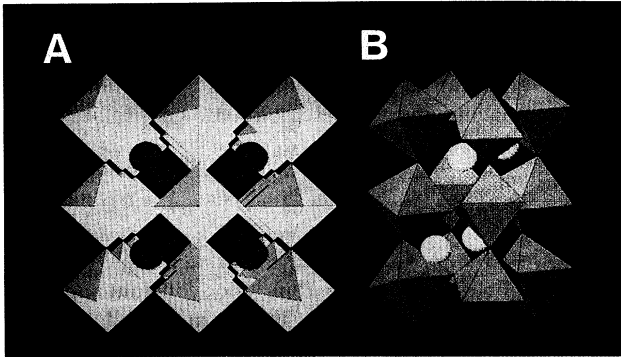


FIG. 1. Hypothetical cubic ($Pm\bar{3}m$) and orthorhombic ($Pbnm$) phases of MgSiO_3 . Blue [yellow] spheres in (a) [(b)] represent Mg ions. The Si ions are located at the O-octahedral inversion centers.

an antiferroelectric-type displacement of Mg ions (blue [yellow] spheres in Fig. 1(a) [1(b)]) perpendicular to the c axis. This brings the number of atoms per cell and the structural parameters to twenty and ten, respectively. After adjusting the masses to produce similar oscillatory frequencies for strains and ions, the search for the LDA lowest enthalpy state [12,13] with $Pbnm$ symmetry proceeded by means of efficient "downhill" minimizations. Whenever a component of the generalized acceleration $\ddot{\mathbf{s}} = (\ddot{\mathbf{q}}_i, \ddot{\epsilon}_{jk})$ with $i=1, \dots, N$, and j and $k=1,3$ changed sign, the corresponding velocity component was zeroed. This strategy guarantees that the final structure's internal virial pressure is equal to that externally imposed. The optimizations required \approx twenty steps to obtain structural parameters with four significant digits, after which the forces and the differences between the internal and the external pressures were reduced to $\approx 10^{-6}$ Ry/ a_0 and 10^{-6} Ry/ a_0^3 , respectively. Figure 2 illustrates a typical dynamical evolution of these parameters, while Table I displays their zero pressure values and compares them to experimental ones [14]. The overall agreement is very good; in particular, the theoretical lattice parameters a , b , and c are consistently smaller by $\approx 1\%$, which is an excellent agreement. Because of the large degree of structural freedom, one might wonder whether there are other metastable structures with this symmetry. We approach this question pragmatically and conduct several optimizations at zero pressure starting from different configurations including one very close to the cubic perovskite. Only one final configuration has been found. This suggests the absence of other metastable configurations

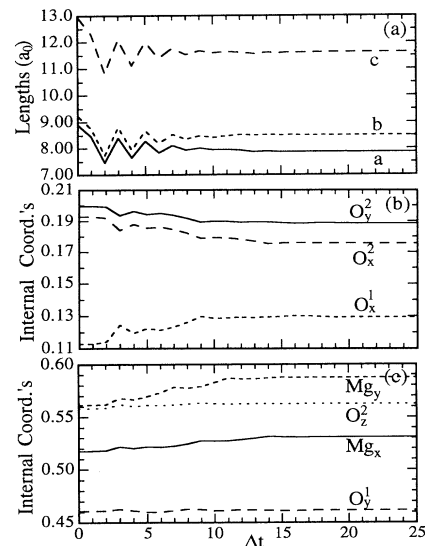


FIG. 2. Typical dynamical evolution of the (a) lattice and (b),(c) internal parameters of the $Pbnm$ phase. In this example the zero pressure structure has been subjected to an applied pressure of 150 GPa. Converged values are obtained in ≈ 20 MD steps.

TABLE I. Experimental [14] and theoretical parameters of the zero pressure $Pbnm$ phase. The primitive vectors are, respectively, $\mathbf{a}=a\hat{x}$, $\mathbf{b}=b\hat{y}$, $\mathbf{c}=c\hat{z}$. This phase (4 MgSiO_3) has Si atoms located at $(\frac{1}{2}, 0, 0)$, $(\frac{1}{2}, 0, \frac{1}{2})$, $(0, \frac{1}{2}, 0)$, and $(0, \frac{1}{2}, \frac{1}{2})$, Mg's at $\pm(\text{Mg}_x, \text{Mg}_y, \frac{1}{4})$, $\pm(\frac{1}{2} - \text{Mg}_x, \text{Mg}_y + \frac{1}{2}, \frac{1}{4})$, and two sets of inequivalent O's at $\pm(\text{O}_x^1, \text{O}_y^1, \frac{1}{4})$, $\pm(\frac{1}{2} - \text{O}_x^1, \text{O}_y^1 + \frac{1}{2}, \frac{1}{4})$ and $\pm(\text{O}_x^2, \text{O}_y^2, \text{O}_z^2)$, $\pm(\frac{1}{2} - \text{O}_x^2, \text{O}_y^2 + \frac{1}{2}, \frac{1}{2} - \text{O}_z^2)$, $\pm(\text{O}_x^2, \text{O}_y^2, \text{O}_z^2 + \frac{1}{2})$, $\pm(\frac{1}{2} + \text{O}_x^2, \frac{1}{2} - \text{O}_y^2, \text{O}_z^2)$. The calculated zero pressure lattice parameter of the $Pm3m$ is 3.472 Å (in contrast to 3.48 [28]). The fourth column gives the equivalent parameters of the $Pm3m$ phase described in terms of an equivalent $Pbnm$ supercell.

	Calc. ($Pbnm$)	Expt. ($Pbnm$)	Calc. ($Pm3m$)
a	4.711	4.777	4.909
b	4.880	4.927	4.909
c	6.851	6.898	6.942
Mg_x	0.5174	0.5131	0.500
Mg_y	0.5614	0.5563	0.500
O_x^1	0.1128	0.1031	0.000
O_y^1	0.4608	0.4654	0.500
O_x^2	0.1928	0.1953	0.250
O_y^2	0.1995	0.2010	0.250
O_z^2	0.5582	0.5510	0.500

within this space group and the instability of the hypothetical cubic phase, as previously suggested by a semiempirical lattice dynamics study [15].

Because of its implications for the structure of the Earth's lower mantle, the behavior of MgSiO_3 under compression has been an issue of great concern. This region can only be probed by seismological tomography [16], the interpretation of which depends entirely on information inferred from high pressure diamond anvil (DA) cell experiments or theoretical materials modeling [11,17,18]. A precise determination of this mineral's equation of state up to pressures typical of this region can have important geophysical implications. The possible existence of other stable phases at high pressures is another related issue. Although DA experiments [14, 19–22] indicate an increasing degree of orthorhombic distortion with pressure, and no evidence is found for a transition up to ≈ 100 GPa and ambient temperatures, the possibility of a temperature aided transition to a more symmetrical phase at lower mantle pressures still seems to be an open question. Comparative crystal chemistry [23] has speculated the possibility of a stable $Pm3m$ phase, and MD simulations using an ionic force field model [24] indicate the $Pbnm$ phase undergoes a temperature-induced transition to the $Pm3m$ before melting and above 10 GPa. These evidences suggest the cubic phase is not the most sensible alternative structure at high pressures and temperatures [11].

Our results, summarized in Figs. 3 and 4, reveal the following trends: (1) The orthorhombic axes have different compressibilities [Figs. 3(c)–3(e)], among which the a axis is the most compressible followed by c and b , as

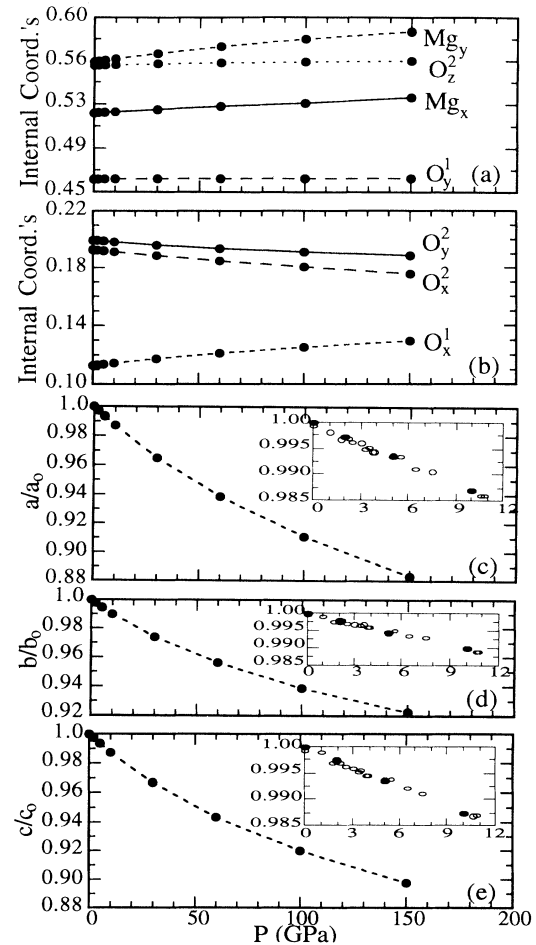


FIG. 3. Pressure dependence of structural parameters for the $Pbnm$ phase. (a) and (b) show the internal ones, while (c), (d), and (e) show the rescaled Bravais lattice parameters a/a_0 , b/b_0 , and c/c_0 , where a_0 , b_0 , c_0 are zero pressure values. The insets show experimental results of Ross and Hazen [14] (○) and of ours (●).

observed in single crystal measurements [14]. This trend becomes more enhanced at lower mantle pressures, and differs from that inferred by a previous potential induced breathing model calculation [25]. (2) The internal parameters vary continuously [Figs. 3(a) and 3(b)] and no change in trend is observed under compression. These imply increasing antiferroelectric displacements of Mg ions, increasing octahedral tilt angles, and a decreasing degree of octahedral distortions [26]. (3) A third-order fit to the Birch-Murnaghan's equation of state [20], of the calculated volume versus pressure relation produces similar bulk moduli for both phases. These and their pressure derivatives are $K_0=259$ and 258 GPa and $K'_0=3.9$ and 4.0 for the $Pbnm$ and cubic phases, respectively. The $Pbnm$ phase's value is within the range spanned by interlaboratory measurements (from 243 [27] to 266 GPa [20]). The $Pm3m$ phase's bulk modulus

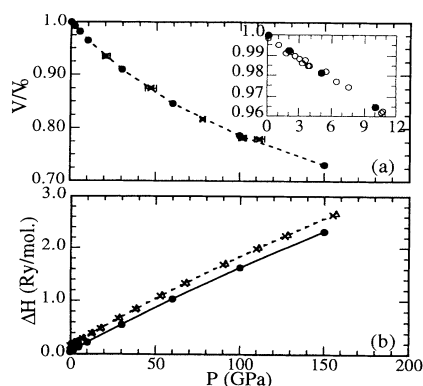


FIG. 4. (a) Pressure dependence of the (*Pbnm*) phase's rescaled volume V/V_0 where V_0 is the zero pressure value. (\times) with error bars are from Knittle and Jeanloz [20], while those in the inset are from Ross and Hazen [14] (\circ) and from ours (\bullet). (b) Change in enthalpy ($H - H_0$), where H_0 is the zero pressure value for the *Pbnm* phase (\bullet). \times and \triangle are results for the cubic phase obtained using 1 and 4 special k points, respectively.

differs slightly from that estimated by an *ab initio* full-potential linear augmented-plane-wave study [28] ($K_0 = 279$ GPa and $K'_0 = 3.4$). (4) Finally, the stability of the *Pbnm* phase with respect to the cubic *Pm3m* perovskite increases with pressure from 1.50 eV/molecule at zero pressure to 3.54 eV/molecule at 150 GPa [Fig. 4(b)]. This fact imposes boundaries on the free energy differences necessary for such a transition, and theoretical estimates of the phonon spectra and related thermodynamical quantities at high pressures in both phases could be of great value.

In summary, we have developed a constant pressure *ab initio* MD algorithm with variable cell shape and applied it to predict the behavior under pressure of the major Earth-forming mineral phase MgSiO_3 perovskite. The stability of this phase is shown to increase with pressure with respect to the cubic perovskite, discarding the possibility of such a transition at mantle pressures, except perhaps at very high temperatures.

We thank N. Ross, R. Angel, and V. Heine for invaluable comments. This work was supported by SERC (R.M.W.) and NERC (G.D.P.) of the United Kingdom. We also acknowledge initial support (R.M.W.) from the Division of Materials Sciences, U.S. Department of Energy, under Contract No. DE-AC02-76CH00016.

[1] R. Car and M. Parrinello, Phys. Rev. Lett. **55**, 2471 (1985).

- [2] M. Parrinello and A. Rahman, Phys. Rev. Lett. **45**, 1196 (1980).
- [3] R. M. Wentzcovitch, Phys. Rev. B **44**, 2358 (1991).
- [4] R. M. Wentzcovitch and J. L. Martins, Solid State Commun. **78**, 831 (1991); R. M. Wentzcovitch *et al.*, Phys. Rev. B **45**, 11 372 (1992).
- [5] L. Stixrude, R. J. Hemley, Y. Fei, and H. K. Mao, Science **257**, 1099 (1992).
- [6] M. L. Cohen, Phys. Scr. **T1**, 5 (1982).
- [7] T. Arias *et al.*, Phys. Rev. B **45**, 1538 (1992); D. M. Bylander and L. Kleinman, Phys. Rev. B **45**, 9663 (1992).
- [8] In formal elasticity theory, the Lagrangian strain ϵ is a symmetric function $\epsilon: \epsilon = \frac{1}{2}(\epsilon + \epsilon^T + \epsilon\epsilon^T)$. For small deformations, ϵ is the symmetric version of ϵ .
- [9] O. H. Nielsen and R. Martin, Phys. Rev. B **32**, 3780 (1985).
- [10] The proof follows by induction from Eqs. (2a), (2b), and (3).
- [11] R. Hemley and R. Cohen, Annu. Rev. Earth Planet. Sci. **20**, 553 (1992).
- [12] We have used soft separable pseudopotentials [13] and a plane-wave (PW) cutoff $E_{PW} = 70$ Ry (≈ 2900 PW's/unit). We have chosen 1 and 2 equivalent special k points in the IBZ's of the cubic and orthorhombic phases, respectively.
- [13] N. Troullier and J. L. Martins, Phys. Rev. B **43**, 1993 (1991); D. M. Ceperley and B. J. Alder, Phys. Rev. Lett. **45**, 1196 (1980); J. P. Perdew and A. Zunger, Phys. Rev. B **23**, 5048 (1981).
- [14] N. L. Ross and R. M. Hazen, Phys. Chem. Minerals **16**, 415 (1989).
- [15] R. Hemley *et al.*, Phys. Chem. Minerals **14**, 2 (1987).
- [16] J. H. Woodhouse and A. M. Dziewonski, Philos. Trans. R. Soc. London A **328**, 291 (1989).
- [17] A. Navrotsky and D. J. Weidner, *Perovskite a Structure of Great Interest for Geophysics and Material Science* (American Geophysics Union, Washington, DC, 1989).
- [18] G. D. Price, A. Wall, and S. C. Parker, Philos. Trans. R. Soc. London A **328**, 391 (1989).
- [19] T. Yagi *et al.*, in *Advances in Physical Geochemistry*, edited by S. K. Saxena (Springer, Berlin, 1982), p. 317.
- [20] E. Knittle and R. Jeanloz, Science **235**, 668 (1987).
- [21] Y. Kudoh *et al.*, Phys. Chem. Minerals **14**, 350 (1987).
- [22] H. K. Mao *et al.*, J. Geophys. Res. **96**, 8069 (1991).
- [23] D. Andrault and J. P. Poirier, Phys. Chem. Minerals **18**, 91 (1991).
- [24] M. Matsui and G. D. Price, Nature (London) **351**, 735 (1991).
- [25] R. Cohen, Geophys. Res. Lett. **14**, 1053 (1987).
- [26] R. Wentzcovitch and G. D. Price (to be published).
- [27] See A. Yeganeh-Haeri *et al.*, in *Perovskite a Structure of Great Interest for Geophysics and Material Science* (Ref. [17]).
- [28] See R. E. Cohen *et al.*, in *Perovskite a Structure of Great Interest for Geophysics and Material Science* (Ref. [17]).

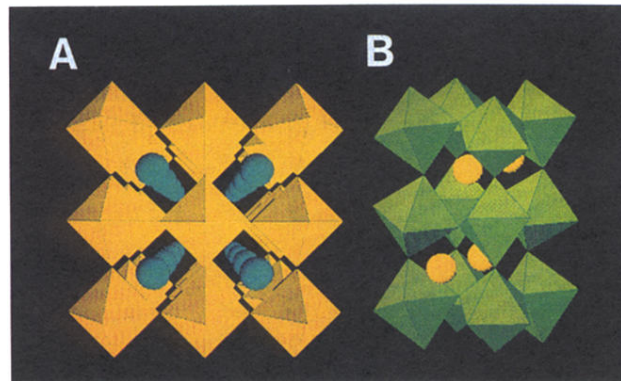


FIG. 1. Hypothetical cubic ($Pm\bar{3}m$) and orthorhombic ($Pbnm$) phases of $MgSiO_3$. Blue [yellow] spheres in (a) [(b)] represent Mg ions. The Si ions are located at the O-octahedral inversion centers.